Hindawi
Journal of Food Biochemistry
Volume 2023, Article ID 5547108, 14 pages
https://doi.org/10.1155/2023/5547108

Research Article

Isochlorogenic Acid C Restrains Erk/JNK/NF-κB Signaling to Alleviate Inflammatory Response and Promote Cell Apoptosis

Yang Liu,[1] **Jiang Liang**,[2] **Qian Ding**,[1] **Changjun Xu**,[1] **Ming Liu**,[1] **and Changfu Yang**[1]

[1]*School of Basic Medicine, Guizhou University of Traditional Chinese Medicine, Guiyang 550025, Guizhou, China*
[2]*First Affiliated Hospital, Guizhou University of Traditional Chinese Medicine, Guiyang 550025, Guizhou, China*

Correspondence should be addressed to Ming Liu; liuming339@gzy.edu.cn and Changfu Yang; yangchangfu251@gzy.edu.cn

Received 16 December 2022; Revised 22 January 2023; Accepted 30 January 2023; Published 20 February 2023

Academic Editor: Jae Young Je

Copyright © 2023 Yang Liu et al. This is an open access article distributed under the Creative Commons Attribution License, which permits unrestricted use, distribution, and reproduction in any medium, provided the original work is properly cited.

Isochlorogenic acid C (ICAC) is found in a variety of natural foods and medicinal plant materials. This study aims to validate the biological activity of isochlorogenic acid C in limiting inflammation by the Erk/JNK/NF-κB pathway. In this study, TNF-α-induced human fibroblast-like synoviocytes and collagen-induced arthritis animal models were used to perceive the potential anti-inflammation mechanism of ICAC. The role of isochlorogenic acid C was evaluated by observing the migration, invasion ability, and apoptotic activity of TNF-α-induced fibroblast-like synoviocytes cells in humans and analysing foot swelling, joint index, and histopathological changes in a collagen-induced RA animal model. The results reveal that ICAC inhibited the proliferation of human fibroblast-like synoviocytes and promoted their apoptosis. ICAC also blocked the nuclear transfer of NF-κB, Erk, and JNK. It was observed that ICAC significantly inhibited the degree of posterior foot swelling in CIA, reducing arthritis scores, bone tissue injury, and articular synovitis. ICAC may promote cell apoptosis and inhibit the hyperactivation of inflammatory cells to alleviate inflammation-induced synovial proliferation through the Erk/JNK/NF-κB pathway.

1. Introduction

Isochlorogenic acid C is a phenolic compound produced by plants, a natural product of quinic acid and caffeine ester condensation, found in various fruits, vegetables, coffee, and spices [1]. It is also found in *Artemisia capillaris* Thunb., *Lonicera japonica*, *Eclipta prostrata*, and other homology of medicine, food, or medicinal plants. Its various biological activities have been demonstrated; for example, isochlorogenic acid C alleviates high-fat diet-induced hyperlipemia by promoting cholesterol reverse transport [2] or isochlorogenic acid C prevents enterovirus infection by regulating the redox homeostasis of glutathione [3]. Inflammation is one of the main target research areas for biomedical researchers, which includes a variety of cellular processes [4, 5]. Rheumatoid arthritis (RA) is an autoimmune disease associated with inflammatory synovial hyperplasia, which easily causes joint swelling and joint cartilage damage with deformity [6]. Early active anti-inflammatory treatment is used to prevent the destruction of joint bone and reduce the rate of disability [7]. In patients with rheumatoid arthritis, joint tissue is typically infiltrated by immune cells, for instance, T cells, B cells, and macrophages, which produce various proinflammatory cytokines such as Erk, JNK, or NF-κB that promote inflammatory responses. The synovial fibroblast is stimulated by inflammation and has strong proliferative and invasive abilities [8]. Earlier studies have shown that activation of ERK, JNK, or NF-κB in human fibroblast-like synoviocytes is essential for IL-1-induced intercellular adhesion molecule expression and leukocyte adhesion [9]. ERK activation in T cells from RA patients was a risk factor [10]. Research on therapeutic drugs for autoimmune diseases, effectively inhibiting cytokines and proteases by blocking or weakening the activation of fibroblasts in the synovial membrane, is one of the crucial strategies for the clinical treatment of RA. However, isochlorogenic acid C has not been explored for its efficacy and mechanism via Erk/JNK/NF-κB signaling against rheumatoid arthritis. This study offers further insight into the development and application of isochlorogenic acid

C after intervention in a cell model and collagen-induced arthritis animal through the preparation of collagen-induced arthritis (collagen-induced arthritis, CIA) rats and TNF-α-induced human fibroblast-like synoviocytes.

2. Materials and Methods

2.1. Chemicals and Reagents. Isochlorogenic acid C (ICAC), with a purity of 98%, was purchased from Desite Biotechnology Co., Ltd. (Lot: 1092320232, Chengdu, China). Matrigel, SDS-PAGE gel kit, phosphate buffer saline (PBS), microscope slides, cover glass, crystal violet stain solution, and glycerin jelly were purchased from Solarbio Science & Technology Co., Ltd. (Lot: 356234, P1200, P1010, YA0172, YA0770, G1064, and S2150, Beijing, China). Dimethylbenzene and anhydrous ethanol were purchased from Kemiou Chemical Reagent Co., Ltd. (Lot: 20070182 and 214393, Tianjin, China). Rat IL-1β ELISA kit, Rat IL-6 ELISA kit, Rat TNF-α ELISA kit, Rat IFN-γ ELISA kit, Rat CXCL1 ELISA kit, Rat IL-17/IL-17A ELISA kit, Human IL-1β ELISA kit, Human IL-18 ELISA kit, Human MIP-1α ELISA kit, and Human MCP-1 ELISA kit were purchased from Neobioscience (Lot: ERC007, ERC003, ERC102a, ERC101g, ERC008, ERC170, EHC002b, EHC127, EHC112a, EHC113, Shenzhen, China). Caspase 1 Antibody and Cleaved-Caspase 1 p20 Antibody were purchased from Affinity Biosciences (Lot: AF5418 and AF4005, Liyang, China). The Anti-NLRP3 antibody, Anti-COX1 antibody, and Anti-COX2 antibody were purchased from Abcam (Lot: ab263899, ab109025, and ab179800, Shanghai, China). Human fibroblast-like synoviocytes were purchased from Jennio Biotech Co., Ltd. (Lot: 342165554, Guangzhou, China). Cell Counting kit-8 (CCK-8), Rabbit Anti-NF-κB p65 antibody, Rabbit Anti-RANKL antibody, Rabbit Anti-β-Actin antibody, Rabbit Anti-Bax antibody, Rabbit Anti-Bcl-2 antibody, Rabbit Anti-IκB α antibody, Rabbit Anti-phospho-Erk1/2 (Thr202 + Tyr204) antibody, Rabbit Anti-Erk1/2 antibody, Rabbit Anti-JNK1 + JNK2 + JNK3 antibody, Rabbit Anti-Phospho-JNK1/2/3 (T183 + T183 + T221) antibody, and Rabbit Anti-Caspase-3 antibody were purchased from Bioss (Lot: BA00208, bs-20355R, bs-0747R, bs-0061R, bs-0127R, bs-20351R, bs-1287R, bs-3016R, bsm-2637R, bs-2592R, bsm-4163R, and bs-0081R, Beijing, China). Phospho-NF-κB p65 Rabbit mAb, Phospho-IκBαRabbit mAb, and Cleaved-Caspase-3 Rabbit mAb were purchased from CST (Lot: #3033, #2859, #9664, Shanghai, China). Incomplete Freund's adjuvant was purchased from Sigma-Aldrich Trading Co., Ltd. (Lot: F5506, Shanghai, China). Bovine II type collagen was purchased from Chondrex (Lot: 190078, Washington, USA). Apoptosis and necrosis assay kit, 2-(4-Amidinophenyl)-6-indolecarbamidine dihydrochloride(DAPI), Caspase-3 activity assay kit, Caspase-6 activity assay kit, Caspase-8 activity assay kit, Caspase-9 activity assay kit, immunofluorescence staining kit with FITC-Labeled Goat Anti-Rabbit IgG, Biotin-labeled Goat Anti-Rabbit antibody, electrochemiluminescence (ECL), and hematoxylin-eosin (HE) staining kit were purchased from Beyotime Biotechnology (Lot: C1056, C1005, C1116, C1136, C1152, C1158, P0186, A0277, P0018FS, and C0105S, Shanghai, China). Minute™ animal cell/tissue total protein extraction kit was purchased from Invent Biotechnology Inc. (Lot: SD-001/SN-002, Beijing, China). A microBCA protein assay kit was purchased from Cwbio (Lot: CW2011, Beijing, China). PVDF was purchased from Millipore (Merck, Shanghai, China). Fetal bovine serum (FBS) and Dulbecco's modified Eagle's medium (DMEM) were purchased from Thermo Fisher Technology Co., Ltd. (Lot: 42F3261K and 8121302, Shanghai, China). Transwell was purchased from Corning (Lot: 354234, Shanghai, China) and recombinant human tumor necrosis factor (TNF-α) was purchased from PeproTech (Lot: 014532, Suzhou, China).

2.2. Culture of Human Fibroblast-Like Synoviocyte. Human fibroblast-like synoviocytes were cultured in DMEM high glucose complete medium containing 10% fetal bovine serum at 37°C and 5% CO_2. Trypsin was digested when the cell density was about 80%.

2.3. Cellular Proliferation Detected by CCK-8. Human fibroblast-like synoviocyte cells (5×10^3 cells) were inoculated in 96-well plates with DMEM high glucose complete medium containing 10% fetal bovine serum. After 24 h, the broth was replaced with fresh medium, and a control group and an ICAC group were set up. Different concentrations of ICAC (0 μM, 50 μM, 100 μM, 200 μM, 400 μM, and 800 μM) were added and repeated in triplicate. CCK-8 (10 μL) was added to each well of every group and incubated at 37°C and 5% CO_2 for 48 h. After incubation for 4 h, the absorbance value was detected at 450 nm.

In addition, cells (5×10^3 cells) were inoculated in 96-well plates, and DMEM high glucose complete medium with 10% fetal bovine serum was added. After 24 h, the broth was replaced with fresh medium, and control, model, and ICAC groups were set up. In the model group, 20 μg/L TNF-α and ICAC of different concentrations were added in triplicate. After 48 h of incubation at 37°C with 5% CO_2, 10 μL CCK-8 was added to each well. After 4 h of incubation, the absorbance was recorded at 450 nm.

2.4. Transwell Migration and Invasion Assays. The effects of ICAC on the migration and invasion of human fibroblast-like synoviocyte cells were studied using a Transwell chamber. Cells (2×10^3 cells) and DMEM high glucose complete medium containing 20% fetal bovine serum (600 μL) were added into the upper and lower Transwell chambers, respectively. Cells were cotreated with ICAC for 48 h in the presence of TNF-α (20 μg/L). Migration to the membrane cells was calculated in six randomly selected areas with the microscope. Similar invasion assays were conducted by adding a Matrigel gel before adding cells to the upper chamber. After 48 h, the chamber membrane was fixed with 4% paraformaldehyde for 30 min and stained with a crystal violet staining solution.

2.5. Immunofluorescence Staining Analysis. Human fibroblast-like synoviocytes were digested using trypsin, and the excess trypsin was washed away by PBS. Cells

(3×10^3 cells) were resuspended in a 24-well plate, and slides of cells were prepared. After 24 h of culture and attachment, the complete medium was replaced. Cells were cotreated with ICAC for 48 h in the presence of TNF-α (20 μg/L). The culture medium was aspirated and washed with PBS thrice. Paraformaldehyde (4%) was fixed for 30 min in the well. After cleaning with PBS thrice, 5% goat serum was added and blocked for 1 hour, and 1 : 100 NF-κBp65, JNK1/2/3, and Erk1/2 antibodies were added directly and incubated overnight at 4°C, washed with PBS thrice. Furthermore, 1 : 300 FITC-labeled goat anti-rabbit IgG was added and incubated for 2 h in the dark, washed with PBS thrice, stained with DAPI, and incubated at room temperature for 10 min in the dark. Three randomly selected fields from each well were photographed and analyzed with a laser confocal microscope.

2.6. Apoptosis Activity Analysis. Firstly, slides were prepared from cultured cells (1×10^3 cells). Anchorage-dependent cells were added and cocultured in cell staining buffer. Hoechst stain and PI stain were cocultured at 4°C for 30 min, washed with PBS, and visualized under a fluorescence microscope. Secondly, the apoptotic activity of human fibroblast-like synoviocyte cells was detected by the caspase-3, 6, 8, and 9 activity assay kit. Cells were digested with trypsin and washed with PBS. Cells of 4×10^6 were inoculated on a T25 cell culture bottle with DMEM high glucose complete medium supplemented with 10% fetal bovine serum. Cells were cotreated with ICAC for 48 h in the presence of TNF-α (20 μg/L). The culture medium was absorbed, the cells were digested with trypsin, and they were centrifuged at 600g and 4°C for 5 min. The lysate from the corresponding kit was added at low temperature for 30 min and centrifuged at 4°C, 20000g for 15 min. The absorbance OD was detected by adding the reaction solution and incubating for 2 h at 37°C.

2.7. IL-1β, IL-18, MIP-1α, and MCP-1 Secretion Content in Cell Supernatant. The digested human fibroblast-like synoviocytes were adjusted to 3×10^5 and inoculated in 6-well plates. Cells were cotreated with ICAC in the presence of TNF-α (20 μg/L) for 48 h. The cell culture medium was collected to detect the OD value according to the ELISA protocol. Firstly, the standard curve for detection was made. Secondly, the samples and the corresponding antibody detection working liquid were added in the 96-well plate and incubated at room temperature away from light. After adding the color developing agent for color development, the contents of IL-1β, IL-18, MIP-1α, and MCP-1 in the cell supernatant were calculated.

2.8. Animals. Specific pathogen-free (SPF) Sprague-Dawley (SD) male rats, weighing 180–220 g and 6–9 weeks old, purchased from Tianqin Biological Co., Ltd. (Hunan, China), bred by the Animal Laboratory Center of Guizhou University of Traditional Chinese Medicine at room temperature 25°C and humidity 45–55%. The animals had free access to standard food and drinking water during the experiment. The Animal Ethics Committee of the Guizhou University of Chinese Medicine approved the experiment plan. The experimental process shall conform to the implementation provisions of the National Regulations on the Administration of Medical Laboratory Animals.

2.9. Collagen-Induced Arthritis. After one week of adaptive feeding, SPF SD rats were divided randomly into the control group ($n = 10$) and the model group ($n = 30$) by the random number table method. The collagen and incomplete Freund's adjuvants were mixed into 2 mg/mL emulsion at the volume ratio of 1 : 1. The model group was respectively injected with 0.4 mL emulsion subcutaneously in the tail root for the first immunization on the 1st day. On the 14th day, 0.2 ml of emulsion was injected for a second immunization. The swelling of rat foot joints was observed and rated 0 to 4 according to the severity of swelling (0 rated no swelling; one rated mild swelling of both feet; two rated moderate swelling of bilateral metatarsal and toes; three rated severe swelling of bilateral metatarsal toes; and four rated total swelling of bilateral metatarsal toes and ankle joint or deformity; a rate above one is randomized to receive drug treatment). After the successful induction of the model, the rats were assigned randomly to the model group: the ICAC 50 mg/kg group and the 100 mg/kg group, with ten rats in each group. After grouping, the animals received the indicated drugs intragastrically for 35 consecutive days. Meanwhile, the control and model groups were given sodium carboxymethyl cellulose. Arthritis index scores were recorded every seven days. Animal weight was recorded, and a rat foot volume measuring instrument was used to measure the degree of double hind limb swelling in rats in each group. The formula (swelling degree = thickness after induction − thickness before induction) was used, and statistical analysis was performed. Isoflurane gas anesthesia was used on the last day of the experiment, micro-CT was used to obtain images of the foot to construct three-dimensional images, and EDTA-K3 anticoagulant was used to collect blood from the abdominal aorta. The spleen was dissected and weighed, and organ coefficients were calculated. The synovium of the left joint, the foot, and the spleen was fixed with 4% paraformaldehyde, and the synovium of the right joint was taken for −80°C cryopreservation. After the end of the experiment, isoflurane overdose was anesthetized and euthanized.

2.10. Pathological Analysis of Spleen and Synovium. The spleen and synovium were flushed with tap water for 30 min and immersed in 70%, 80%, 90%, and 100% ethanol for 2 h. The synovium and spleen were soaked in xylene for 10 min and 30 min, respectively. The synovium and spleen were soaked in liquid paraffin for 15 min and 1 h, respectively. Sections were prepared, and the slides of synovium and spleen samples of 4 μm thickness were dewaxed with fresh xylene for 30 min. Slides were immersed in 100%, 90%, 80%, and 70% ethanol for 10 min, soaked in distilled water for 1 min, hematoxylin stained for 10 min, rinsed with tap water for 5 min, stained with eosin for 1 min, soaked in 70% and 90% ethanol for 10 min, and xylene for 10 min, and observed under the microscope.

2.11. Western Blot Analysis in Synovium. Total protein was extracted using columnar centrifugation and quantified by BCA. Separation gel (12%) and gel (5%) concentration gel electrophoresis was prepared. Different concentrations of antibodies were used, including β-actin (1 : 6000), NLRP3 (1 : 500), Caspase-1 (1 : 1000), Cleaved-Caspase-1 (1 : 500), NF-κBp65 (1 : 1000), phospho-NF-κBp65 (1 : 500), IκB-α (1 : 1000), phospho-IκB-α (1 : 500), RANKL (1 : 1000), Erk1/2 (1 : 1000), phospho-Erk1/2 (1 : 500), JNK1/2/3 (1 : 1000), phospho-JNK1/2/3 (1 : 500), COX-1 (1 : 1000), COX-2 (1 : 1000), Caspase-3 (1 : 1000), Cleaved-Caspase-3, Bax (1 : 1000), and Bcl-2 (1 : 1000). After overnight incubation at 4°C, II antibody (1 : 8000) and ECL were added. The experiment was repeated three times. After each PVDF membrane was regenerated with a regenerating agent, an antibody was added for reincubation and development.

2.12. ELISA Assay for Serum. The rat plasma was centrifuged at 3000g for 15 min. The expression of IL-1β, IL-6, TNF-ɑ, IFN-γ, IL-17, and CXCL-1 in the plasma was detected using an ELISA kit according to the manufacturer's protocols.

2.13. Statistical Analysis. All data from a minimum of three experiments were recorded as mean ± SD. Data were analyzed using GraphPad Prism 9.0 software (GraphPad Software, Santiago, USA) based on a one-way ANOVA with Dunnett's multiple comparisons test. A value of $P < 0.05$ was considered significant.

3. Results

3.1. ICAC Inhibits Proliferation of Fibroblast-Like Synoviocyte. After 48 h of incubation of fibroblast-like synoviocytes, the optimal concentration of the drug was determined. Based on this optimal concentration, the subsequent experimental drug concentrations (50, 100, and 200 μM) were determined (Figures 1(a) and 1(b)).

3.2. ICAC Lessens Cell Migration and Invasion. After the incubation of human fibroblast-like synoviocytes for 48 h, TNF-α significantly increased their migration and invasion capacity. The different concentrations of ICAC significantly reduced human fibroblast-like synoviocytes migration and invasion ability compared to TNF-α (Figures 2(a)–2(d)).

3.3. ICAC Restrain Nuclear Translocation of NF-κBp65, JNK, and Erk Proteins in Cells. After 48 h of incubation, NF-κBp65, JNK, and Erk protein expression levels in human fibroblast-like synoviocytes were all higher than those in the control group. Different concentrations of ICAC significantly inhibited the overexpression and nuclear translocation of NF-κBp65, JNK, and Erk proteins in the cells (Figures 3–5).

3.4. ICAC Enhances Apoptosis Activity in Cells. In the control group, TNF-α apoptosis activity was not expressed in cells. However, ICAC at different concentrations significantly promoted cell apoptosis activity (Figure 6).

3.5. ICAC Lessens IL-1β, IL-18, MIP-1α, and MCP-1 Secretion in Cells. TNF-α promoted the expression of IL-1β, IL-18, MIP-1α, and MCP-1 when compared with the control cells. The addition of ICAC to the cells significantly inhibited the overexpression of these proteins (Figures 7(a)–7(d)).

3.6. ICAC Decreases Inflammatory Swelling of Feet. The following results show the effect of ICAC on animal weight and arthritis scores. After 35 days of drug treatment, there was no significant body weight difference between the groups (Figure 8(a)). The arthritis score remained high in the CIA group compared to the control group, and ICAC significantly reduced the collagen-induced arthritis score in rats (Figure 8(b)). Figures 8(c) and 8(d) show the effect of ICAC on the inflammatory swelling of the rear feet of CIA rats. After five weeks of drug intervention, the foot swelling was significantly reduced in CIA rats.

3.7. ICAC Protects Bone Tissue and Synovium. After five weeks of drug intervention, ICAC significantly increased bone content in the CIA animal models (Figures 9(a), 9(b), and 9(d)). The collagen-induced immune response resulted in the disappearance of the normal synovium structures, fibroblast proliferation, lymphocytic infiltration within the synovium, and a high score of synovial pathology. After five weeks of ICAC intervention, the synovial cell proliferation and lymphocyte infiltration were significantly reduced, and the synovial pathology score was low (Figures 9(c) and 9(e)).

3.8. ICAC Influences Spleen and Visceral Coefficients. After five weeks of the consecutive drug intervention, the CIA visceral coefficient significantly increased, compared with the control group, while ICAC significantly reduced the visceral coefficient of CIA in the spleen (Figure 10(b)). Furthermore, pathological changes in the spleen after HE staining showed that the control group had more secondary lymphoid follicles, and the periarterial lymphatic sheath was arranged into cylinders. In CIA, secondary lymphatic follicles in the spleen atrophied and disappeared. Only a few primary lymphatic follicles were contained, and the periarterial lymphatic sheath was reduced. Compared to CIA, the ICAC-L and ICAC-H contained more primary lymphatic follicles in the spleen, while with the periarterial lymphatic sheaths was increased (Figure 10(a)).

3.9. ICAC Restrain Inflammatory and Apoptosis Factors. The synovial infiltration of lymphocytes, such as monocytes, T cells, and B cells, produced mononuclear and chemotactic factors that stimulated synovial cell proliferation and promoted the entry of leukocytes into joints. NF-κB regulated gene expression affects innate and adaptive immunity, inflammation, stress response, B cell development, and lymphoid organ formation. In the classic signaling pathway, NF-κB protein binds to and is inhibited by IκB protein, and inflammasomes have been implicated in various autoinflammatory and autoimmune diseases. NLRP3, Caspase-1, Cleaved-Caspase-1, phospho-IκB-α, NF-κBp65, phospho-

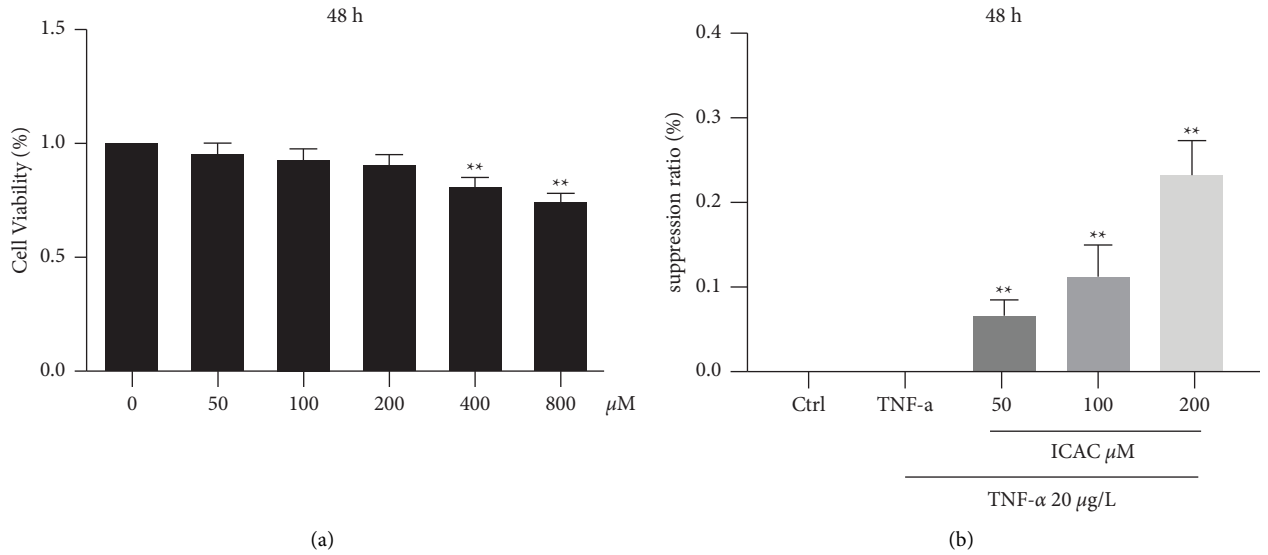

Figure 1: Effects of ICAC on growth and suppression ratio of human fibroblast-like synoviocytes. Different concentrations of ICAC were added in cells and incubated for 48 h. 20 μg/L TNF-a were added to human fibroblast-like synoviocytes to promote their proliferation, and the inhibition rate of ICAC on proliferating cells was analyzed after incubating for 48 h. (a) Cell viability of human fibroblast-like synoviocytes; (b) the suppression ratio of human fibroblast-like synoviocytes. ($^{**}P < 0.01$ vs. TNF-a group, $n = 3$).

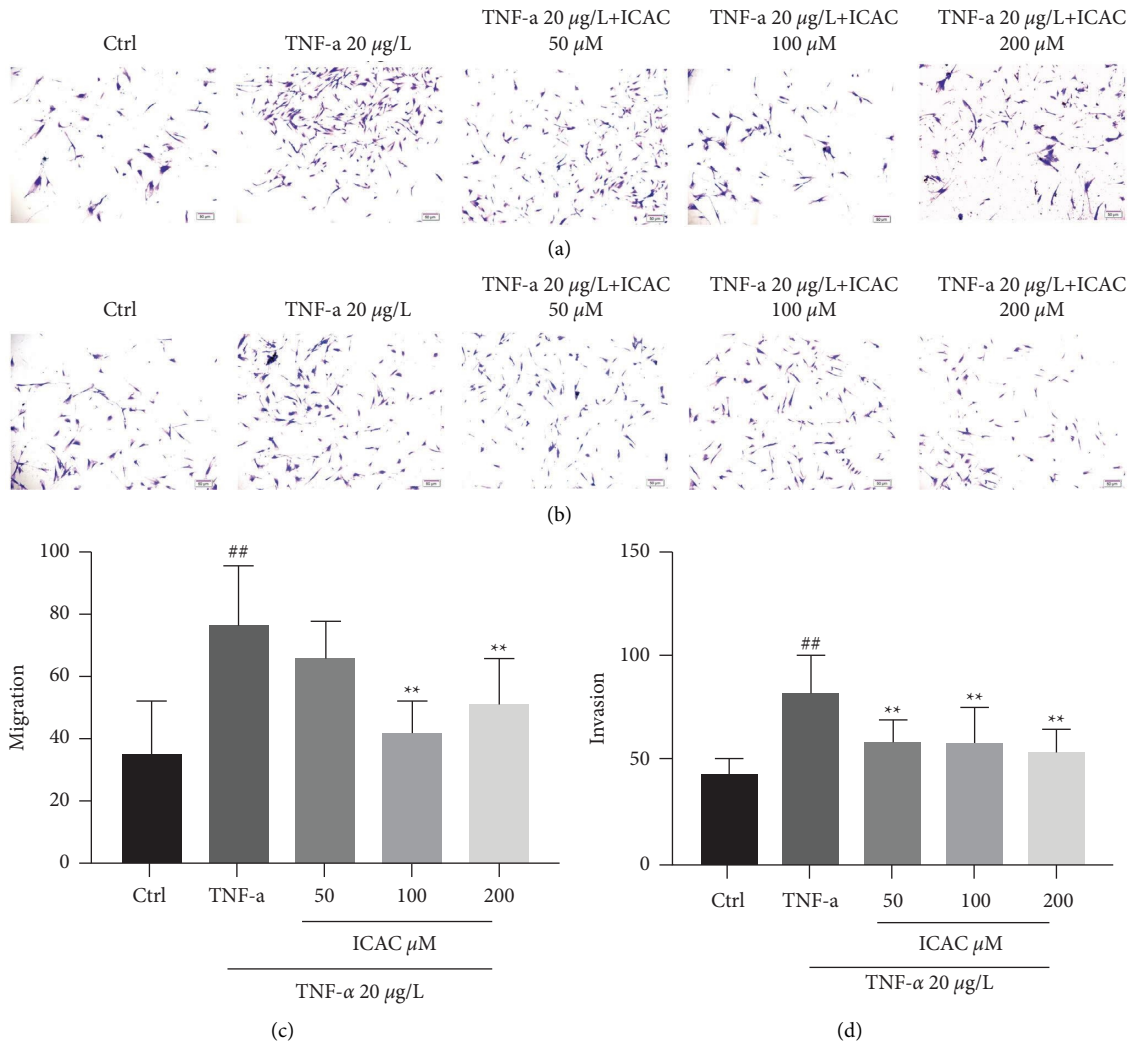

Figure 2: Effects of ICAC on migration and invasion ability of human fibroblast-like synoviocytes. 20 μg/L TNF-a and different concentrations of ICAC were added in cells and incubated for 48 h. (a, c) Migration count of human fibroblast-like synoviocytes; (b, d) invasion count of human fibroblast-like synoviocytes. ($^{\#\#}P < 0.01$ vs. control group; $^{**}P < 0.01$ vs. TNF-a group. $n = 6$).

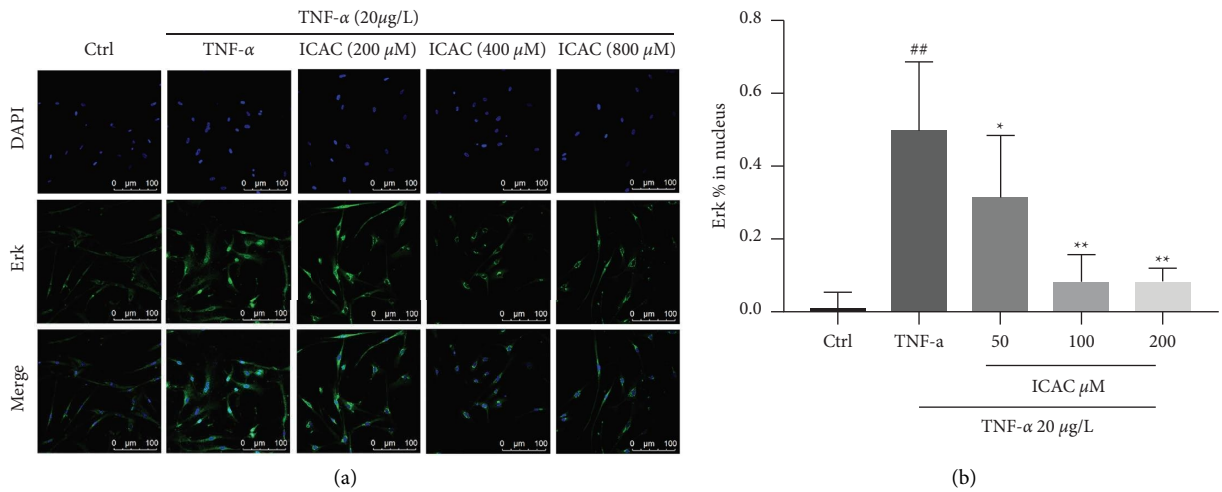

(a) (b)

Figure 3: Effects of ICAC on expression of Erk protein in human fibroblast-like synoviocytes. 20 μg/L TNF-a and different concentrations of ICAC were added in cells and incubated for 48 h. (a, b) The expression of Erk protein in 10 to 20 fibroblast-like synoviocytes. ($^{\#\#}P < 0.01$ vs. control group; $P < 0.05$ and $^{**}P < 0.01$ vs. TNF-a group, $n = 3$).

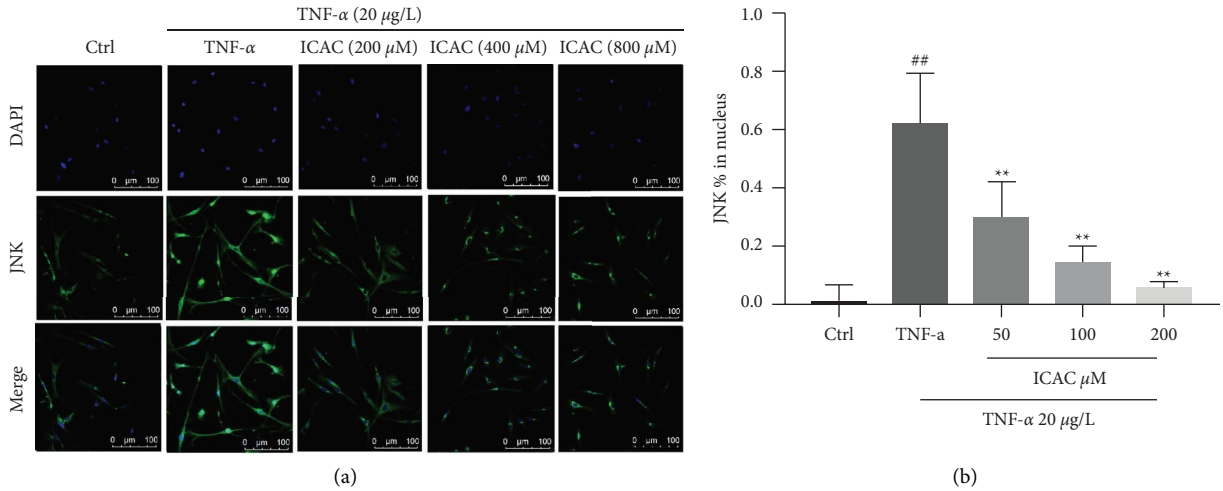

(a) (b)

Figure 4: Effects of ICAC on expression of JNK protein in human fibroblast-like synoviocytes. 20 μg/L TNF-a and different concentrations of ICAC were added in cells and incubated for 48 h. (a, b) The expression of JNK protein in 10 to 20 fibroblast-like synoviocytes. ($^{\#\#}P < 0.01$ vs. control group; $^{**}P < 0.01$ vs. TNF-a group, $n = 3$).

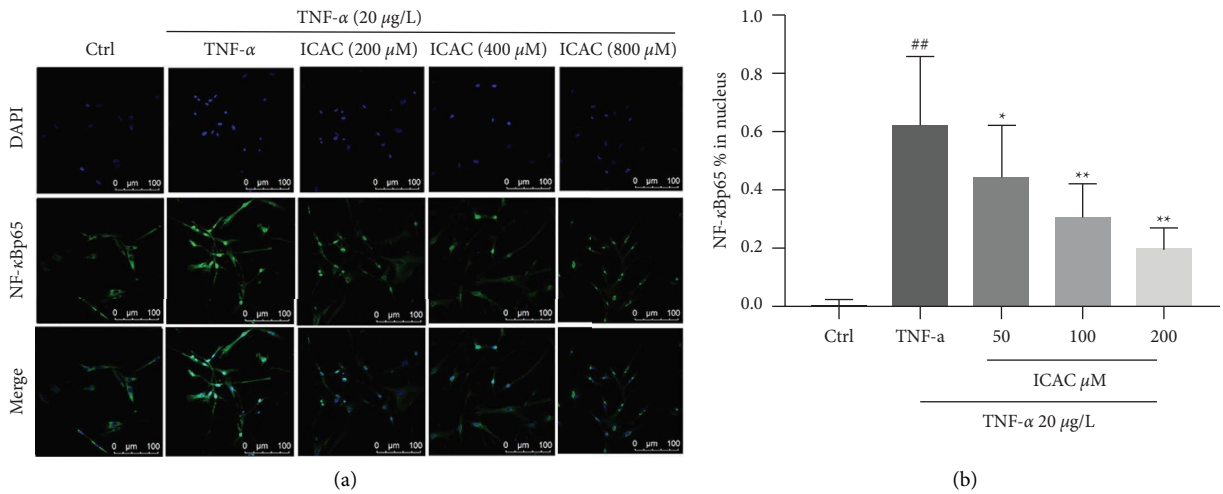

(a) (b)

Figure 5: Effects of ICAC on expression of NF-κBp65 protein in human fibroblast-like synoviocytes. 20 μg/L TNF-a and different concentrations of ICAC were added in cells and incubated for 48 h. (a, b) The expression of NF-κBp65 protein in 10 to 20 fibroblast-like synoviocytes. ($^{\#\#}P < 0.01$ vs. control group; $P < 0.05$ and $^{**}P < 0.01$ vs. TNF-a group, $n = 3$).

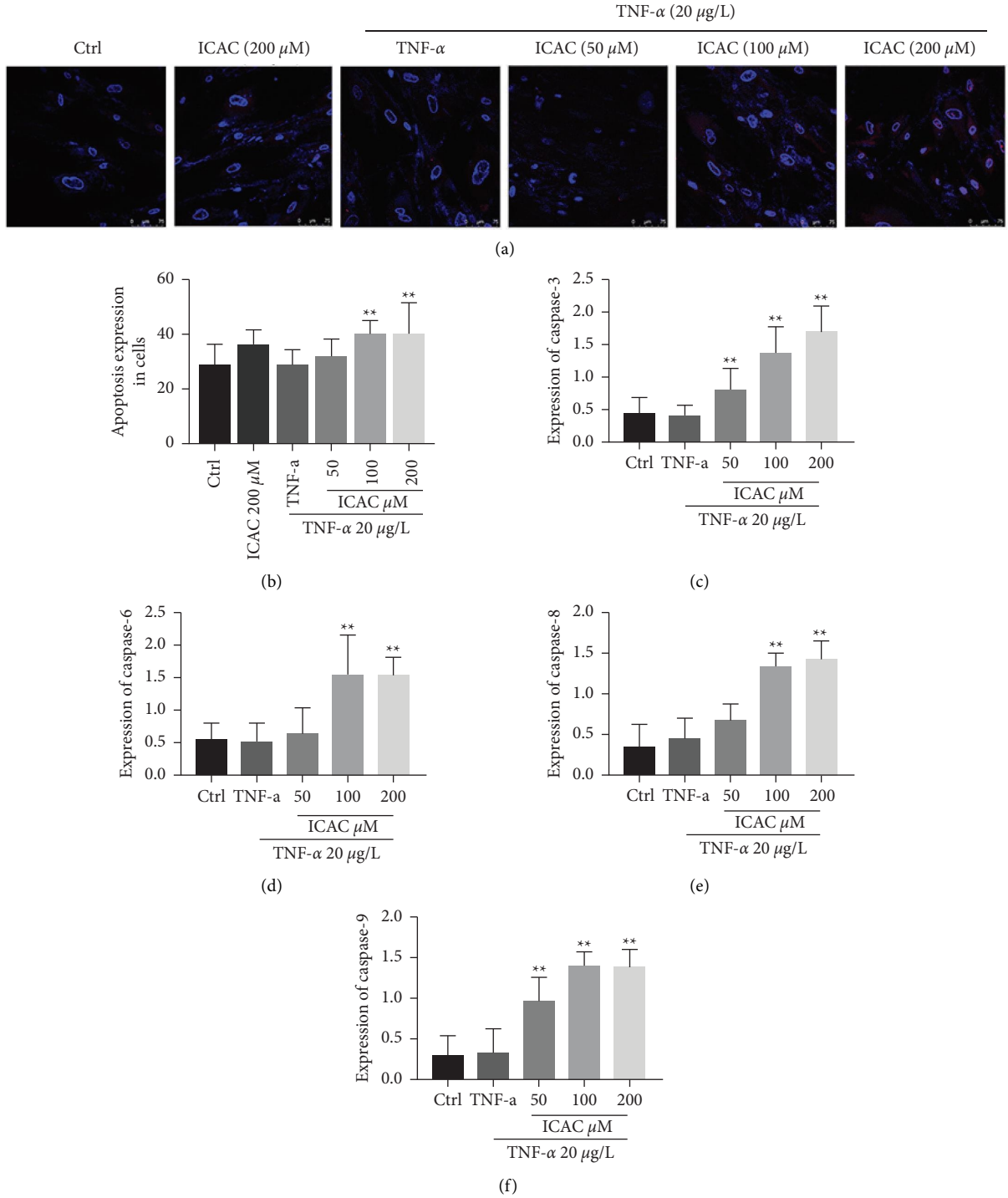

Figure 6: Effects of ICAC on apoptosis expression in human fibroblast-like synoviocytes. 20 μg/L TNF-a and different concentrations of ICAC were added in cells and incubated for 48 h. (a, b) The expression of apoptosis cells by Hoechst 33342-propidium iodide staining in 10 to 20 fibroblast-like synoviocytes. (c–f) Effect of ICAC on Caspase-3, Caspase-6, Caspase-8, and Caspase-9 expressions in human fibroblast-like synoviocytes. (** $P < 0.01$ vs. TNF-a group, $n = 3$).

NF-κBp65, RANKL, Erk1/2, phospho-Erk1/2, JNK1/2/3, phospho-JNK1/2/3, COX-1, and COX-2 increased in CIA than the control group, and IκB-α performed the opposite way. ICAC significantly inhibited the overexpression of these proteins as compared to CIA, but IκB-α was opposite to other proteins. Apoptosis proteins such as Caspase-3, Cleaved-Caspase-3, and Bax were upregulated in ICAC than in CIA, but Bcl-2 was downregulated (Figures 11(a)–11(d)).

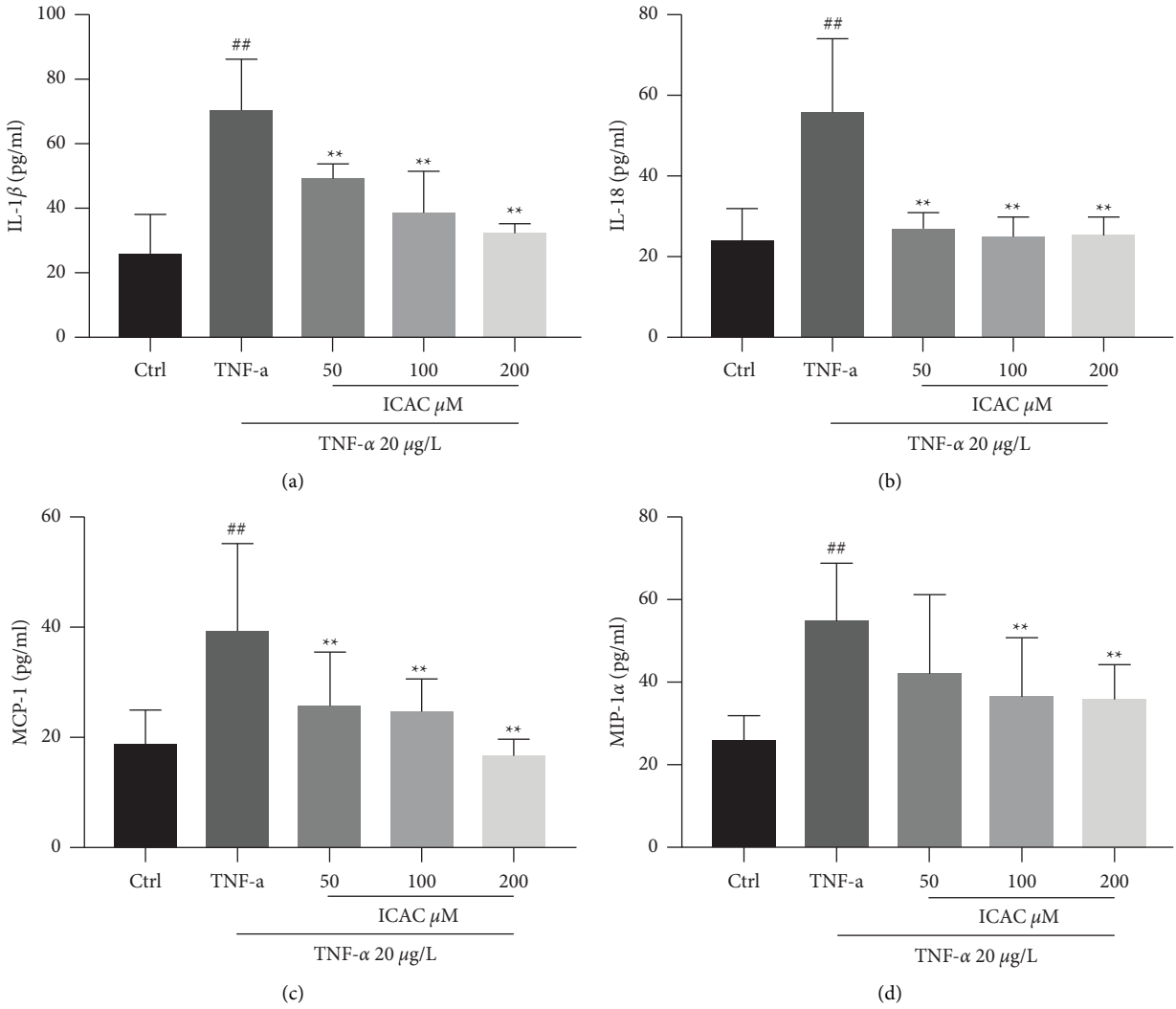

Figure 7: Effects of ICAC on expressions of IL-1β, IL-18, MIP-1α, and MCP-1 in cell culture supernatant (a–d). ($^{\#\#}P < 0.01$ vs. control group; $^{**}P < 0.01$ vs. TNF-a group, $n = 6$).

3.10. ICAC Inhibits Inflammatory Cytokines in Plasma. After five weeks, plasma from each group was detected using ELISA, in which IL-1β, IL-6, TNF-α, IFN-γ, CXCL1, and IL-17/IL-17A were upregulated in CIA than the control group and downregulated in ICAC (Figures 12(a)–12(f)). These phenomena indicate that ICAC may potentially inhibit these inflammatory factors.

4. Discussion

As products of the caffeic acid derivative, compounds with similar chemical structures have been reported to have multiple pharmacological activities. 3, 5-, or 4, 5-dicaffeoylquinic acid may improve islet function in type 2 diabetic mice, and 3, 5-dicaffeoylquinic acid has a strong antibacterial effect [11]. Studies have confirmed that fibroblast-like synoviocytes are direct effector cells of rheumatoid arthritis, and their high activation, secretion of inflammatory factors, and blocking of apoptosis are essential mechanisms leading to inflammation and tissue damage in rheumatoid arthritis [12]. The inflammasome is an important part of innate immunity, and the NLRP3 inflammasome regulates T cell responses [13]. The involvement of inflammasomes in the pathogenesis of RA was confirmed in various studies on genetic association in animal models and patient samples [14]. It was also closely related to inflammatory bowel disease, gout, and other inflammatory autoimmune diseases [15]. Classical inflammasome pathways are engaged by the oligomerization of pattern-recognition receptors that play a significant role in recognizing pathogen- and damage-associated molecular patterns [16]. The NOD-like receptor family, pyrin domain-containing 3 (NLRP3), is an endogenous and exogenous receptor that senses danger signals [17] and assembles with an apoptosis-associated speck-like protein containing a CARD (ASC) and Caspase-1 to form a multimeric protein called the NLRP3 inflammasome. The outflow of potassium ions (K^+) is a typical marker of NLRP3 inflammasome activation and is also required for apoptotic assembly. The NLRP3 inflammasome is an

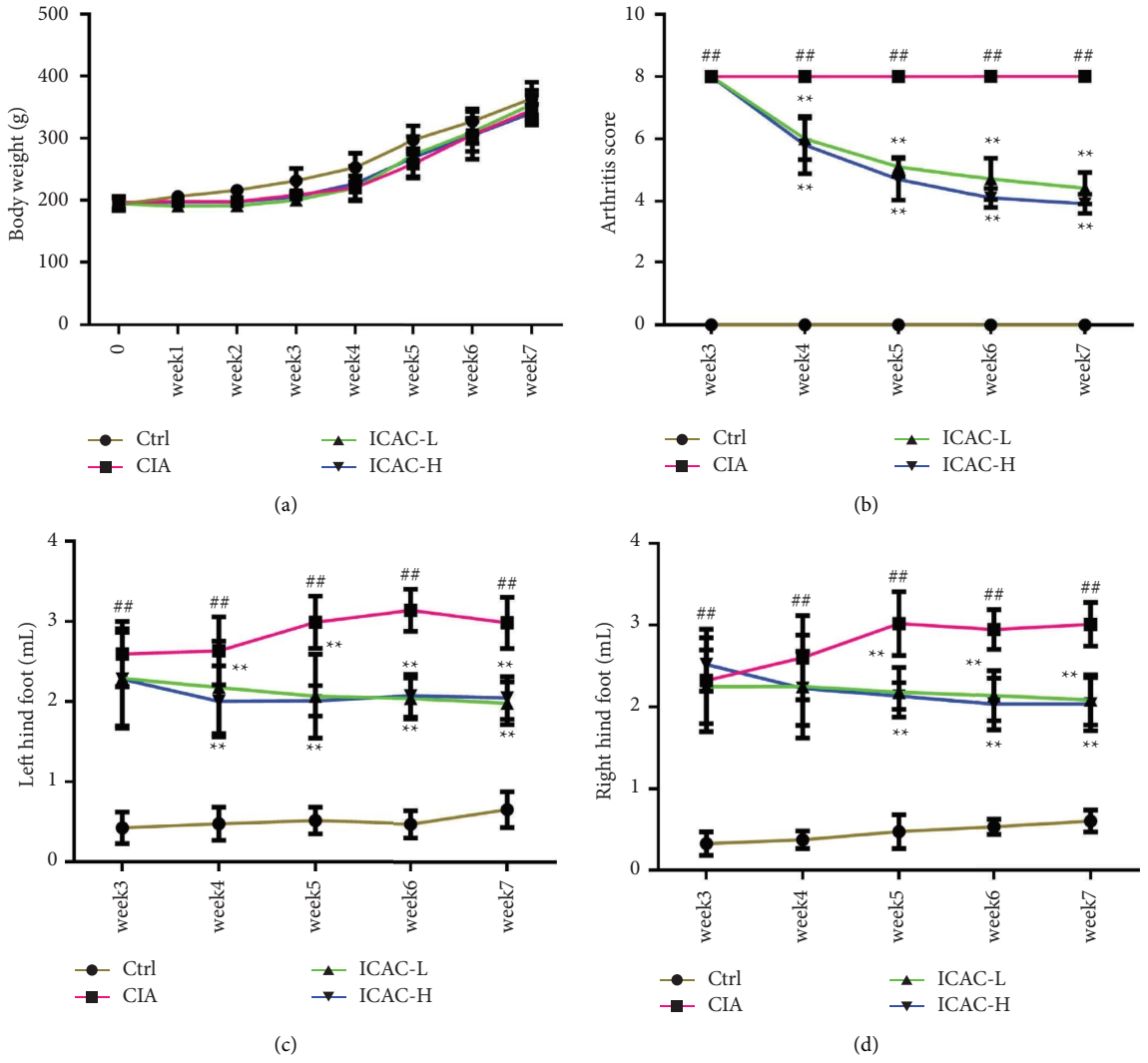

Figure 8: Effects of ICAC on animal growth and inflammatory swelling of feet. 40 male Wistar rats were randomly divided into 4 groups according to body weight: control (vehicle), CIA (collagen-induced arthritis), CIA-ICAC-L (50 mg/kg), and CIA-ICAC-H (100 mg/kg). After successful replication of the CIA animal model, intervention was continued for 5 weeks, body weight was measured and recorded once a week, arthritis score was performed once a week, and volume after collagen-induced swelling was measured once a week. (a) The growth curve of rats ($n = 10$); (b) the severity of arthritis by the arthritis score; (c) the left hind foot ($n = 10$); (d) the right hind foot ($^{\#\#}P < 0.01$ vs. control group; $^{**}P < 0.01$ vs. CIA group, $n = 10$).

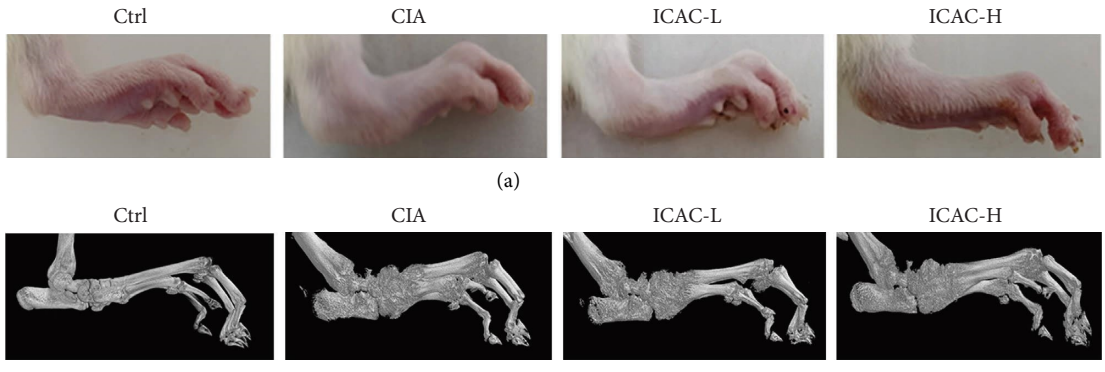

Figure 9: Continued.

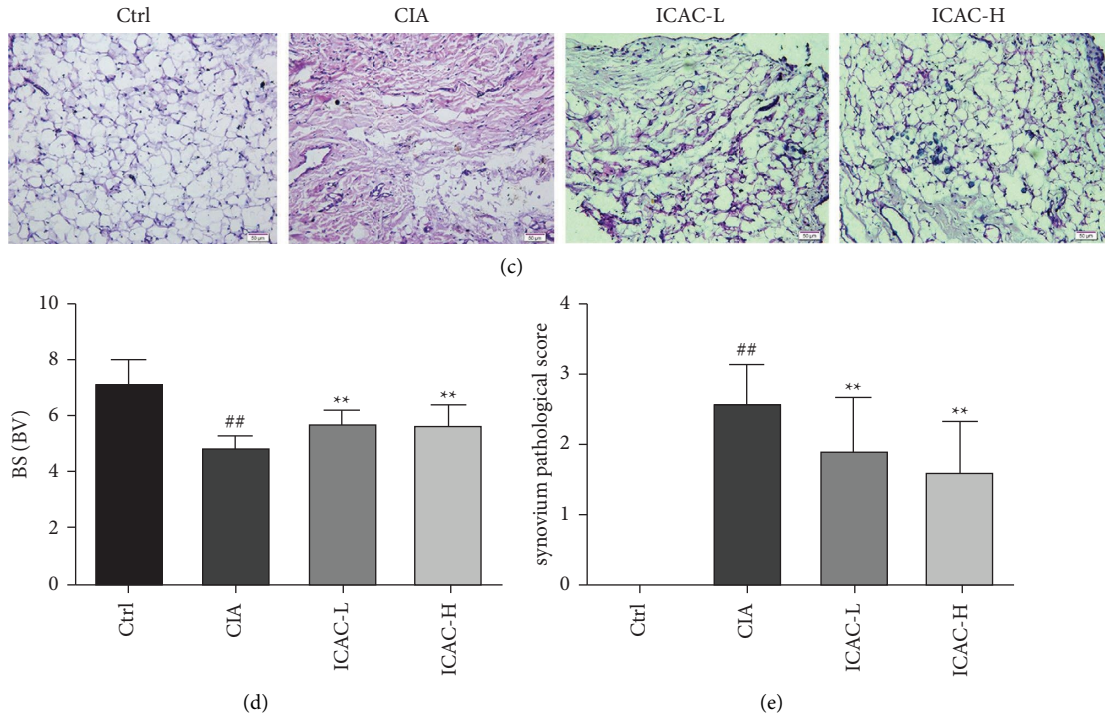

Figure 9: Effects of ICAC on animal bone tissue and synovium. (a) After collagen induction, paw swelling was evident in the model group compared with the control group, but significantly decreased after ICAC treatment; (b) micro-CT was used to take photos of the left hind foot to construct three-dimensional images. Images showed significant bone destruction in all rats after collagen stimulation compared with control mice; (c) HE stained the synovium of the left joint; (d) ICAC treatment was able to significantly reduce the paw bone destruction. Bone surface (BS) to bone volume (BV) ratio in the left hind foot ($n = 10$); (e) the synovium pathological score of the left joint after HE staining. The number of cell proliferation and the degree of tissue fibrosis were assessed under an ordinary microscope, and the assessment of pathological features was 0 (normal), 1 (mild), 2 (moderate), and 3 (severe) ($^{\#\#}P < 0.01$ vs. control group; $^{**}P < 0.01$ vs. CIA group, $n = 10$).

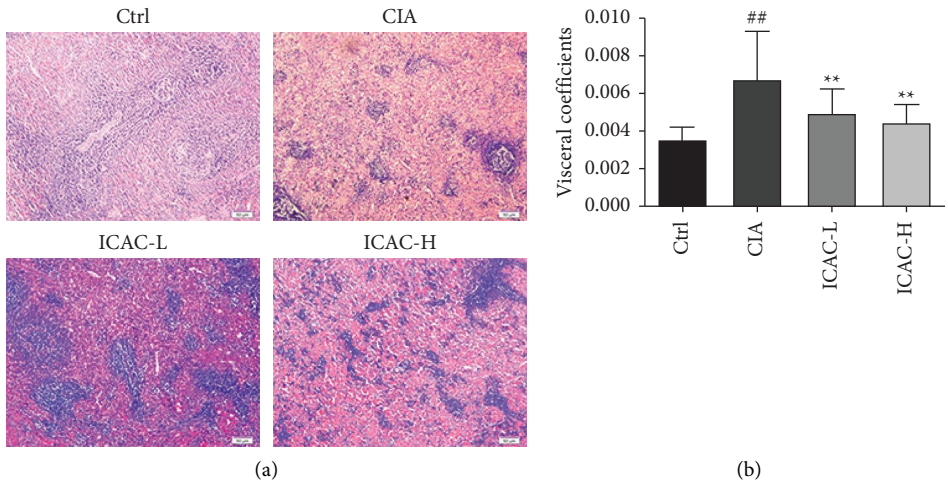

Figure 10: Effects of ICAC on spleen and visceral coefficients. (a) Pathological changes in the spleen. (b) Changes in the visceral coefficients of the spleen ($^{\#\#}P < 0.01$ vs. control group; $^{**}P < 0.01$ vs. CIA group, $n = 10$).

important cellular sensor and effector that stabilizes cell membranes and initiates stress responses [18]. NLRP3 is generally self-inhibited when exposed to various extracellular K^+, Cl^-, and Ca^{2+} fluxes, lysosomal damage, mitochondrial dysfunction, and reactive oxygen species production. NLRP3, pro-caspase-1, ASC assembly and promotes self-activation of Pro-Caspaese-1 into Caspase-1, forming isomer with enzyme activity, which cleaves pro-IL-1β and Pro-IL-18 into IL-1β and IL-18. Two important features of Caspase-1 activation are cell death and cytokine

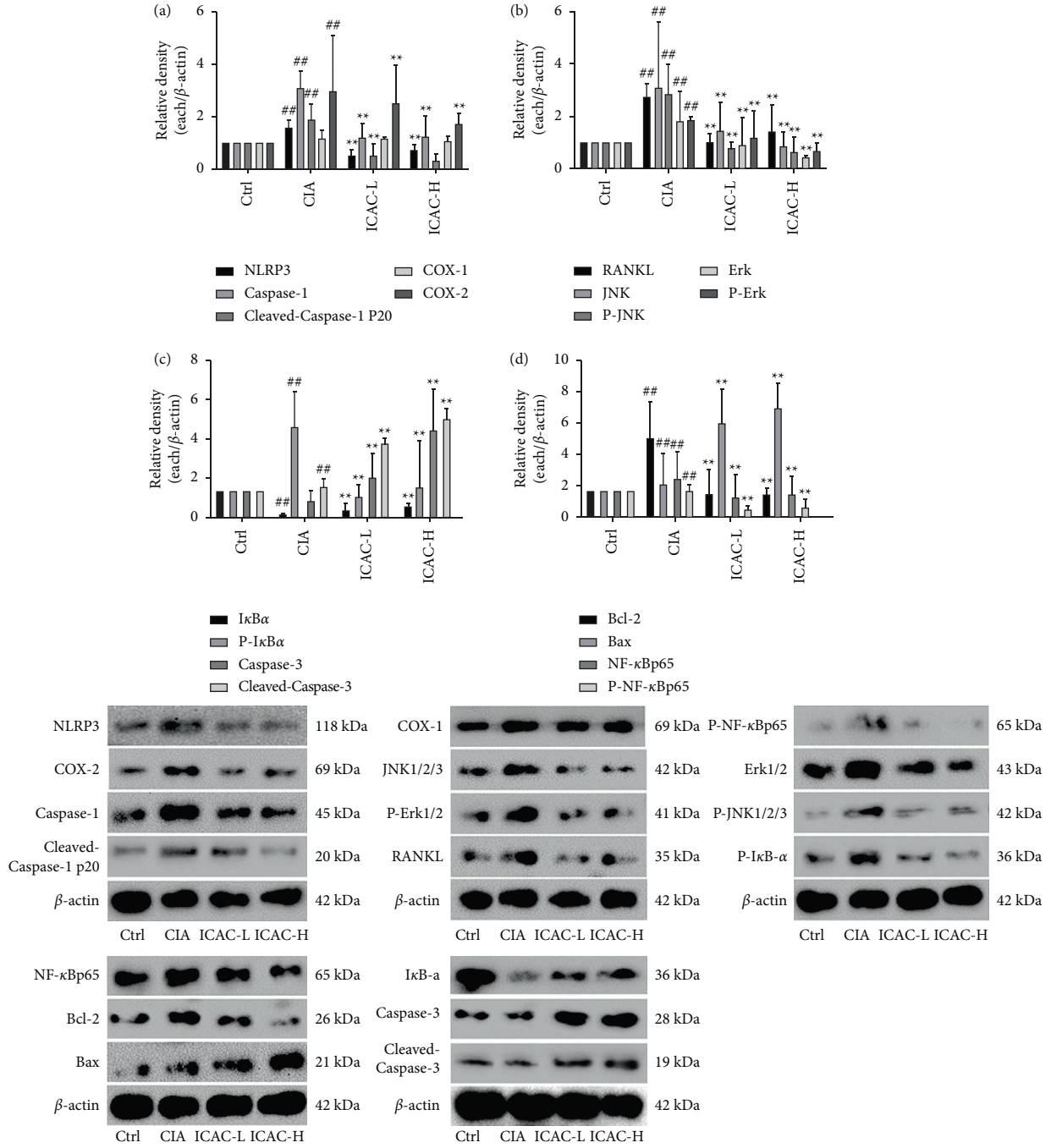

Figure 11: ICAC reduced the expression of NLRP3, Caspase-1, Cleaved-Caspase-1, phospho-IkB-a, NF-κBp65, phospho-NF-κBp65, RANKL, ERK1/2, phospho-ERK1/2, JNK1/2/3, phospho-JNK1/2/3, and COX-2, and increased the expression of IkB-a in synovium (a–c). The apoptosis proteins expression levels of Caspase-3, Cleaved-Caspase-3, and Bax were upregulated, but Bcl-2 was downregulated (c-d). The proteins were detected by western blotting. ($^{\#\#}P < 0.01$ vs. control group; $^{**}P < 0.01$ vs. CIA group, $n = 3$).

release. IL-1β binds to IL-1R to activate NF-κB signaling pathways and promote inflammatory gene expression and T cell activation [19]. IL-1β participates in joint destruction in RA, promotes synovial fibroblast cells' pathological proliferation, releases matrix metalloproteinases that degrade cartilage, stimulates bone absorption, and also inhibits bone and cartilage repair [20]. IL-18 plays a vital role in RA patients' bone and cartilage destruction. IL-18 can induce synovial macrophages to produce TNF-α. Granulocyte-macrophage colony-stimulating factor expression acts on articular chondrocytes. Besides, synovial tissue regulates cell response and participates in joint degeneration. The expression of NLRP3, Caspase-1, and Cleaved-Caspase-1 was examined in the animal synovial membrane, and ICAC significantly inhibited their expression. ELISA examined these inflammatory factors of IL-1β and CXCL1 in animal plasma under the influence of ICAC. Compared with the model group, ICAC could

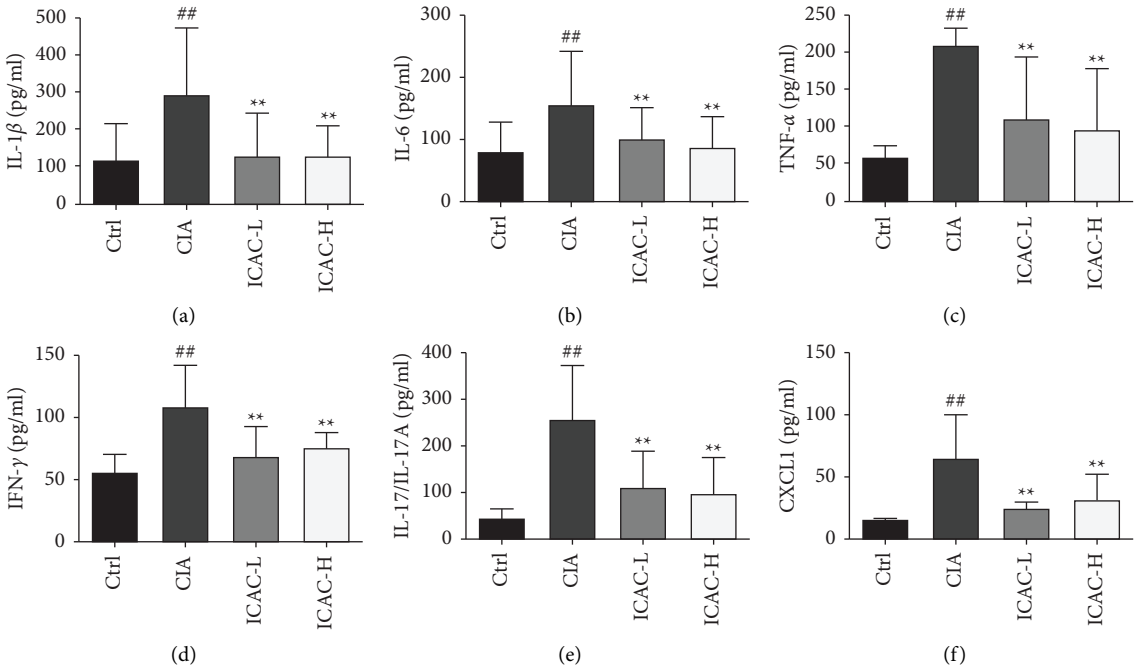

Figure 12: ICAC reduced the production of IL-1β (a), IL-6 (b), TNF-a (c), IFN-y (d), IL-17/IL-17 (e), and CXCL1 (f) in CIA animal plasma. ($^{\#\#}P < 0.01$ vs. control group; $^{**}P < 0.01$ vs. CIA group, $n = 10$).

decrease the expression of IL-1β and CXCL1. The secretion levels of IL-1β and IL-18 in the culture medium of cells were also examined, confirming that ICAC inhibits the expression of these two inflammatory factors. This evidence suggests that NLRP3 can be regulated by ICAC and inhibit downstream inflammation. NF-κB activation is closely related to the excessive proliferation and inflammation of fibroblast synovial cells, which regulate various cellular transduction processes. This includes an increase in anti-apoptotic genes expression, inhibition of apoptotic regulatory molecules expression (P53, Bax, and Fas), promoting the release of proliferogenic growth factors, maintaining cytokines of chronic inflammation in synovial membranes, and promoting migration of adhesion molecules contributing to inflamed sites and enhanced invasive properties [21, 22]. The most common subunit is the NF-κB p65/p50 heterodimer, which is generally nonactivated upon binding to its inhibitory protein IκB. Various factors stimulated the heterodimer, phosphorylation of NF-κB p65, and degradation of IκB, leading to NF-κB activation. After NF-κB activation, inflammatory injuries aggravated, leading to an imbalance in proliferation and apoptosis in fibroblast-like synoviocyte. We observed intrasynovial NF-κBp65, phospho-NF-κBp65, IκB-α, phospho-IκB-α, RANKL, Caspase-3, Cleaved-Caspase-3, Bax, and Bcl-2 expression in CIA animals, and these proteins are associated with NF-κB signaling and regulation of apoptosis. ICAC inhibits NF-κB signaling expression and promotes the regulation of apoptosis. ICAC significantly inhibited NF-κBp65 nucleation expression in human fibroblast-like synoviocytes cells, further aggravating the apoptosis in human fibroblast-like synoviocytes cells.

At present, studies suggest that immune dysfunction is closely related to the onset of rheumatoid arthritis. Persistent joint inflammation further aggravates immune system dysfunction, abnormal proliferation of pathogenic lymphocytes, and unbalanced environmental homeostasis in T cells [23]. The disorderly function of T cells, especially antigen-presenting and $CD4^+$ T cell interactions, leads to abnormal activation of $CD4^+$ T cells and triggers the imbalance in Th cell subsets. Th1 and Th17 cells release positive feedback to the inflammatory response such as IFN-γ, TNF-α, IL-1, and IL-17. Clinical samples showed significantly elevated IL-17 and TNF-α in RA patients, synergistically activating synovial fibroblast cells, inducing cartilage and fibroblast synovial cell synthesis, secreting inflammatory mediators and promoting synovial inflammatory response and cartilage destruction [24]. Conversely, Th2 and Treg cells release negative feedback on the inflammatory response and inhibit the excessive inflammatory response of rheumatoid arthritis. Moreover, RA Breg dysfunction in peripheral blood was also an important cause of immune tolerance in RA patients. B cells were also one of the vital antigen-presenting cells, together with dendritic cells, activating T cells' secretion of proinflammatory factors or directly leading to joint damage by participating in the pathogenesis of RA. B cells could pass through the B cell receptor in variants of citrulline peptides, form a major histocompatibility complex (MHC), stimulate differentiation of autoreactive T cells into memory T cells and promote their migration to the synovium, regulate dendrite cell function, and activate the autoimmune response [25]. Therefore, we examined the Erk1/2, phospho-Erk1/2, JNK1/2/3, phospho-JNK1/2/3, COX-1, and COX-2 protein

expression. ELISA examined the IFN-γ, TNF-α, IL-6, and IL-17 in animal plasma and MIP-1α and MCP-1 expression in cell culture medium. ICAC significantly inhibited the nucleation and overexpression of these proteins. The phenotypic changes in fibroblast-like synoviocyte cells were examined, and ICAC significantly inhibited the migration and invasion abilities of fibroblast-like synoviocyte cells. Our study confirmed that ICAC improved the pharmacological activity of RA using the collagen-induced rheumatoid arthritis model. After five weeks of uninterrupted administration of ICAC, each animal group showed no significant differences in body weight. It was suggested that ICAC might be low toxic, which was merely speculative and required further toxicology analyses. ICAC was able to reduce the degree of foot swelling in CIA animals significantly. It showed an effect on inhibiting collagen-induced autoimmune inflammation. Disrupted behavior of bone tissue and the pathological proliferation of fibroblast-like synoviocytes were also inhibited effectively. At the same time, the spleen morphology and pathological changes of the CIA animal model were observed. The spleen organ coefficient increased in CIA, but the organ coefficient significantly decreased in drug treatment, and spleen pathology also changed with drug treatment. Overall, morphological characteristics showed that ICAC has a good antagonistic effect on rheumatoid arthritis.

5. Conclusion

Altogether, this study revealed that the ICAC may regulate Erk/JNK/NF-κB signaling to alleviate synovial proliferation and inflammation through cell models and animal models, respectively. This study not only supplements the pharmacological action of ICAC and food applications but also provides a theoretical basis. Of course, there are also shortcomings in this study, which do not make an in-depth analysis of the specific biological effects target of ICAC. Future studies will be further carried out.

Data Availability

All data generated or analyzed during this study are included in this published article.

Additional Points

Many people are dying every year from inflammation caused by different diseases. Although new anti-inflammatory drugs are emerging all the time, their side effects are also very obvious. Therefore, the development of new anti-inflammatory drugs from the diet or medicinal plants has a broad scope. In this study, the cell model and animal model are used to verify the anti-inflammatory mechanism of ICAC. The results show that ICAC can affect the anti-inflammatory effect via Erk/JNK/NF-κB signaling, which provides the basis for further understanding the anti-inflammatory effect of ICAC.

Ethical Approval

The Animal Ethics Committee of the Guizhou University of Tradition Chinese Medicine approved the experiment plan. The experiment process was in line with the implementation rules of the National Management of Medical Experimental Animals.

Conflicts of Interest

The authors declare that they have no conflicts of interest.

Authors' Contributions

Yang Liu was in charge of validation and writing the original draft; Jiang Liang and Qian Ding handled validation; Changjun Xu was in charge of investigation; Changfu Yang was in charge of conceptualization and funding acquisition; and Ming Liu handled formal analysis, writing the review, and editing. Yang Liu, Jiang Liang, and Qian Ding contributed equally to this work and share first authorship.

Acknowledgments

This work was supported by grants from the Science and Technology Fund of Guizhou (no. ZK(2022)473) and (no.(2019)1033) and the Administration of Traditional Chinese Medicine Fund of Guizhou of China (no. QZYYZDK(PY)2021-04).

References

[1] H. Lu, Z. Tian, Y. Cui, Z. Liu, and X. Ma, "Chlorogenic acid: a comprehensive review of the dietary sources, processing effects, bioavailability, beneficial properties, mechanisms of action, and future directions," *Comprehensive Reviews in Food Science and Food Safety*, vol. 19, no. 6, pp. 3130–3158, 2020.

[2] L. Zheng, G. Lin, R. Li et al., "Isochlorogenic acid C alleviates high-fat diet-induced hyperlipemia by promoting cholesterol reverse transport," *Frontiers in Pharmacology*, vol. 13, Article ID 881078, 2022.

[3] Z. Cao, Y. Ding, L. Cao, G. Ding, Z. Wang, and W. Xiao, "Isochlorogenic acid C prevents enterovirus 71 infection via modulating redox homeostasis of glutathione," *Scientific Reports*, vol. 7, no. 1, Article ID 16278, 2017.

[4] P. Arulselvan, M. T. Fard, W. S. Tan et al., "Role of antioxidants and natural products in inflammation," *Oxidative Medicine and Cellular Longevity*, vol. 2016, Article ID 5276130, 2016.

[5] L. Zhao, B.-D. Yuan, J.-L. Zhao et al., "Amelioration of hexavalent chromium-induced bioaccumulation, oxidative stress, tight junction proteins and immune-related signaling factors by Allium mongolicum Regel flavonoids in Ctenopharyngodon idella," *Fish & Shellfish Immunology*, vol. 106, pp. 993–1003, 2020.

[6] D. M. Lee and M. E. Weinblatt, "Rheumatoid arthritis," *The Lancet*, vol. 358, no. 9285, pp. 903–911, 2001.

[7] G. R. Burmester and J. E. Pope, "Novel treatment strategies in rheumatoid arthritis," *The Lancet*, vol. 389, no. 10086, pp. 2338–2348, 2017.

[8] K. M. Doody, N. Bottini, and G. S. Firestein, "Epigenetic alterations in rheumatoid arthritis fibroblast-like synoviocytes," *Epigenomics*, vol. 9, no. 4, pp. 479–492, 2017.

[9] C.-M. Yang, S.-F. Luo, H.-L. Hsieh et al., "Interleukin-1β induces ICAM-1 expression enhancing leukocyte adhesion in human rheumatoid arthritis synovial fibroblasts: involvement of ERK, JNK, AP-1, and NF-κB," *Journal of Cellular Physiology*, vol. 224, no. 2, pp. 516–526, 2010.

[10] K. Singh, P. Deshpande, S. Pryshchep et al., "ERK-dependent T cell receptor threshold calibration in rheumatoid arthritis," *The Journal of Immunology*, vol. 183, no. 12, pp. 8258–8267, 2009.

[11] J. Luo, K. Wang, G. S. Li et al., "3,5-Dicaffeoylquinic acid disperses Aspergillus fumigatus biofilm and enhances fungicidal efficacy of voriconazole and amphotericin B," *Medical Science Monitor*, vol. 24, pp. 427–437, 2018.

[12] E. K. Kim, J.-E. Kwon, S.-Y. Lee et al., "IL-17-mediated mitochondrial dysfunction impairs apoptosis in rheumatoid arthritis synovial fibroblasts through activation of autophagy," *Cell Death & Disease*, vol. 8, no. 1, Article ID e2565, 2017.

[13] C. Venegas and M. T. Heneka, "Inflammasome-mediated innate immunity in Alzheimer's disease," *The FASEB Journal*, vol. 33, no. 12, pp. 13075–13084, 2019.

[14] C. Guo, R. Fu, S. Wang et al., "NLRP3 inflammasome activation contributes to the pathogenesis of rheumatoid arthritis," *Clinical and Experimental Immunology*, vol. 194, no. 2, pp. 231–243, 2018.

[15] Y. Zhen and H. Zhang, "NLRP3 inflammasome and inflammatory bowel disease." *Frontiers in Immunology*, vol. 10, p. 276, 2019.

[16] V. A. K. Rathinam and K. A. Fitzgerald, "Inflammasome complexes: emerging mechanisms and effector functions," *Cell*, vol. 165, no. 4, pp. 792–800, 2016.

[17] S. M. Man and T. D. Kanneganti, "Regulation of inflammasome activation," *Immunological Reviews*, vol. 265, no. 1, 2015.

[18] A. Malik and T. D. Kanneganti, "Inflammasome activation and assembly at a glance," *Journal of Cell Science*, vol. 130, no. 23, pp. 3955–3963, 2017.

[19] I. S. Afonina, Z. Zhong, M. Karin, and R. Beyaert, "Limiting inflammation-the negative regulation of NF-κB and the NLRP3 inflammasome," *Nature Immunology*, vol. 18, no. 8, pp. 861–869, 2017.

[20] C. C. Huang, C.-H. Chiou, S. C. Liu et al., "Melatonin attenuates TNF-α and IL-1β expression in synovial fibroblasts and diminishes cartilage degradation: implications for the treatment of rheumatoid arthritis," *Journal of Pineal Research*, vol. 66, no. 3, Article ID e12560, 2019.

[21] J.-H. Du, M.-Y. Xu, Y. Wang, Z. Lei, Z. Yu, and M.-Y. Li, "Evaluation of Taraxacum mongolicum flavonoids in diets for Channa argus based on growth performance, immune responses, apoptosis and antioxidant defense system under lipopolysaccharide stress," *Fish & Shellfish Immunology*, vol. 131, pp. 1224–1233, 2022.

[22] J. T. Guo, X. Q. Cao, L. L. Wu et al., "Effect of IL-1β on apoptosis of synovial cells in rheumatoid arthritis rats via the NF-κB pathway," *European Review for Medical and Pharmacological Sciences*, vol. 23, no. 23, pp. 10211–10217, 2019.

[23] C. M. Weyand, M. Zeisbrich, and J. J. Goronzy, "Metabolic signatures of T-cells and macrophages in rheumatoid arthritis," *Current Opinion in Immunology*, vol. 46, pp. 112–120, 2017.

[24] I. Serio and F. Tovoli, "Rheumatoid arthritis: new monoclonal antibodies," *Drugs of Today*, vol. 54, no. 3, pp. 219–230, 2018.

[25] S. Fillatreau, "B cells and their cytokine activities implications in human diseases," *Clinical Immunology*, vol. 186, pp. 26–31, 2018.